

ORIGINAL RESEARCH PAPER

# Fracture Toughness of Warm Mix Asphalts Containing Reclaimed Asphalt Pavement

A. Yousefi<sup>a</sup>, S. Pirmohammad<sup>b,\*</sup>, S. Sobhi<sup>c</sup>

<sup>a</sup>Department of Civil Engineering, Iran University of Science and Technology, Tehran, Iran.

<sup>b</sup>Department of Mechanical Engineering, University of Mohaghegh Ardabili, Ardabil, Iran.

<sup>c</sup>Department of Civil Engineering, Babol Noshirvani University of Technology, Babol, Iran.

## Article info

### Article history:

Received 21 June 2020

Received in revised form

10 September 2020

Accepted 16 September 2020

### Keywords:

Asphalt mixture

Reclaimed asphalt pavement

Fracture toughness

Mixed mode I/II

SCB specimen

## Abstract

This paper deals with the fracture toughness of three different asphalt mixtures of HMA (Hot Mix Asphalt), WMA (Warm Mix Asphalt) and WMA-RAP (i.e. mixture of WMA and reclaimed asphalt pavement). Fracture tests were performed on SCB (Semi-Circular Bend) specimens to obtain the fracture properties (i.e. fracture toughness and fracture energy) of asphalt mixtures under three different modes of loading (i.e. pure mode I, pure mode II and mixed mode I/II) at the two test temperatures of  $-15^{\circ}\text{C}$  and  $25^{\circ}\text{C}$ . The results exhibit that the WMA (i.e. WMA and WMA-RAP) mixtures provide greater fracture toughness than the HMA one under any mode of loading and temperature conditions; however, the WMA-RAP shows the highest fracture toughness. Furthermore, the fracture energies of the WMA and WMA-RAP mixtures are higher than the HMA mixture; however, the WMA mixture demonstrates the greatest value of fracture energy compared to other mixtures. Both the fracture toughness and fracture energy of the mixtures at  $-15^{\circ}\text{C}$  are also found to be higher than those at  $25^{\circ}\text{C}$ .

## 1. Introduction

Aggregates and bitumen are blended, transported, placed, and compacted in a heated condition to produce HMA (Hot Mix Asphalt) pavements. On the other hand, in order to produce WMA (Warm Mix Asphalt) concrete, various techniques (i.e. additives and foaming technology) are used to significantly reduce mix production temperature by  $17\text{-}56^{\circ}\text{C}$ . Hence, WMA is a technology of producing asphalt concrete at temperatures lower than the traditional HMA concrete by viscosity reduction or workability enhancement of the mixtures. In general, the temperature that WMA mixtures are produced is about  $100\text{-}140^{\circ}\text{C}$ ; while, for

the HMA ones, it is in the range of  $150\text{-}170^{\circ}\text{C}$ . A reduction in temperature is acquired in the manufacturing of WMA concrete without aggravating its mechanical performance. WMA concrete has many advantages such as reduced greenhouse gas emissions, less energy consumption, longer hauling distances, etc. [1].

One of the rehabilitation techniques of asphalt pavement is asphalt concrete recycling. RAP (Reclaimed Asphalt Pavement) materials are obtained through milling and processing of old asphalt concretes. Millions of tons of asphalt mixtures are acquired from damaged asphalt pavements in the world. The disposal of this waste material in landfills has many problems such as scarcity of landfill areas and environmental reg-

\*Corresponding author: S. Pirmohammad (Associate Professor)

E-mail address: s\_pirmohammad@uma.ac.ir

<http://dx.doi.org/10.22084/jrstan.2020.22325.1153>

ISSN: 2588-2597

ulations. Consequently, the application of RAP in asphalt mixtures is increasing rapidly due to the increase of fuel costs and shortage of intact materials. The use of RAP is a promising way to employ discarded materials to protect environment and reduce expenses of production and construction of asphalt overlays. Previous researches indicate that the use of RAP saves the materials and expenses, and improves performance of asphalt overlays [2]. It is pointed out that there are inherent limitations in the use of high percentages of RAP in asphalt concretes. Since RAP consists of aged bitumen, the utilization of higher percentages of RAP is a main concern in producing asphalt concretes. The addition of higher contents of RAP may produce asphalt concretes with lower values of stiffness [3, 4]. According to Boriack et al. [5], the content of RAP used in asphalt mixture was recommended to be less than 25% in the United States.

Many researches have been carried out in the past years to study different characteristics of asphalt concretes containing RAP materials. For example, Vukosavljevic [6] indicated that the addition of 30% RAP to asphalt mixture reduced its fatigue life. Results of Mannan et al. [7] showed that the addition of 35% RAP decreased the fatigue life. Mangiafico et al. [8] showed that there was an optimum value of 20-40% RAP to incorporate into asphalt concrete for improving its fatigue properties. According to Guo et al. [9], enhancing the amount of RAP in WMA concrete led to the reduction of rutting resistance. Lu and Saleh [10] studied the rutting behavior of WMA mixtures containing different contents of RAP material ranging from 0 to 70%. The results showed that the rutting resistance of WMA concrete improved as the amount of RAP increased. Fakhri and Ahmadi [11] evaluated the influence of RAP on fracture resistance of asphalt concretes. They measured the critical strain energy release rate ( $J_c$ ) of the mixtures, and the results showed that the addition of the RAP materials decreased the fracture resistance. Behroozikhah et al. [12] investigated fatigue behavior of mixtures containing RAP, Sasobit and crumb rubber. The results showed that the use of RAP, crumb rubber and Sasobit simultaneously led to the improvement of the fatigue performance. According to Behnia et al. [13], the use of 30% RAP resulted in the significant reduction of the fracture energy. The results of Mubaraki et al. [14] showed that the flexural strength and mode-I fracture toughness of mixtures containing 40% RAP were greater compared to the mixtures without RAP. In another study, Huang et al. [15] showed that the use of RAP enhanced the tensile strength and fatigue resistance of the mixtures. Ziari et al. [16] added fibers into HMA mixtures containing RAP, and the results revealed that the fibers had positive effect on the fracture behaviour of mixtures.

Cracking is one of the distresses appearing in as-

phalt pavements. Over the past years, researchers have made many attempts to improve fracture resistance of asphalt concretes by using additives, nanomaterials and fibers. For example, Li and Marasteanu [17], Pirmohammad and his coworkers [18-21], Aliha and his coworkers [22, 23], Razmi and Mirsayyar [24] improved the fracture resistance of asphalt concretes by using various additives like styrene-butadiene-styrene and crumb rubber. Pirmohammad and his coworkers [25, 26] and Ziari et al. [27] employed different nanomaterials such as carbon nanotubes, nano- $Fe_2O_3$ , nanoclays and nano- $Al_2O_3$  to explore the cracking performance of asphalt mixtures. Furthermore, several studies [28-31] have been also carried out to investigate the effect of various fibers like jute, kenaf, carbon and basalt. The results revealed that these fibers had a positive effect on the improvement of fracture resistance of asphalt concretes.

As mentioned above, there are many papers discussing the different characteristics of WMA concretes containing RAP. However, a few investigations have been performed on the fracture behavior of this type of asphalt mixtures. Thus, this paper investigates the mixed mode I/II and pure mode II fracture behavior of WMA concretes containing RAP materials by measuring the fracture toughness and fracture energy. The fracture tests are performed using SCB (Semi-Circular Bend) specimen.

## 2. Materials

Asphalt concretes are usually composed of three main components including aggregates, bitumen and air void. However, other materials are sometimes added to them for improving their performance characteristics [32].

In this research, three different asphalt mixtures designated as HMA, WMA and WMA-RAP are prepared according to Superpave mix design. Table 1 displays the compositions and volumetric parameters of these mixtures. Table 2 shows the properties of bitumen, supplied by Pasargad Oil Company, with penetration grade of 60/70. Furthermore, siliceous aggregates with the nominal maximum aggregate size (NMAS) of 19mm are employed. Fig. 1 shows the aggregate gradation for the production of mixtures. The HMA mixture used in this research is composed of the mentioned bitumen and aggregates with an air void content of 4%. The same bitumen, aggregates and air void content together with 3% of Sasobit are employed to prepare the WMA mixture. Likewise, in order to prepare the WMA-RAP mixture, the bitumen, aggregates, 3% air void content and 3% Sasobit together with 25% RAP are used. It is worth noting that this amount of RAP is chosen based on the recommendations of other researchers. As mentioned earlier, there

are inherent limitations in the use of high percentages of RAP in asphalt concretes. According to Boriack et al. [5], the allowable content of RAP is generally under 25% in the United States. Hence, in this research, 25% RAP is incorporated into WMA mixture. It is also pointed out that the RAP material used in the WMA-RAP mixture is obtained from the stockpile of reclaimed asphalt pavement. The field aged bitumen in RAP material is extracted as per ASTM D2172 [33], and is then recovered in accordance with ASTM D5404 [34]. Based on the ignition test, the content of the bitumen in the RAP is 4.9% of the total weight of the RAP material.

It is noticed that the optimum bitumen contents of the HMA, WMA and WMA-RAP mixtures studied in this research are 5.3, 5.6 and 6.1%, respectively. Meanwhile, other volumetric parameters of the mixtures are presented in Table 1.

In order to prepare the mixtures, virgin aggregates are initially dried in an oven at a certain temperature (i.e. 160°C for HMA and 138°C for WMA) for 24 hours. Hot virgin aggregates are then mixed with plain bitumen and Sasobit modified bitumen to produce HMA and WMA mixtures, respectively. Likewise, the RAP material is blended with the mixture of aggregates and modified bitumen to produce WMA-RAP mixture. The final mixtures are cured at the compaction temperature (i.e. 135°C for HMA and 125°C for WMA) for 2 hours. It is noticed that the RAP

material is maintained at the compaction temperature (i.e. 125°C) before blending with the virgin aggregates.

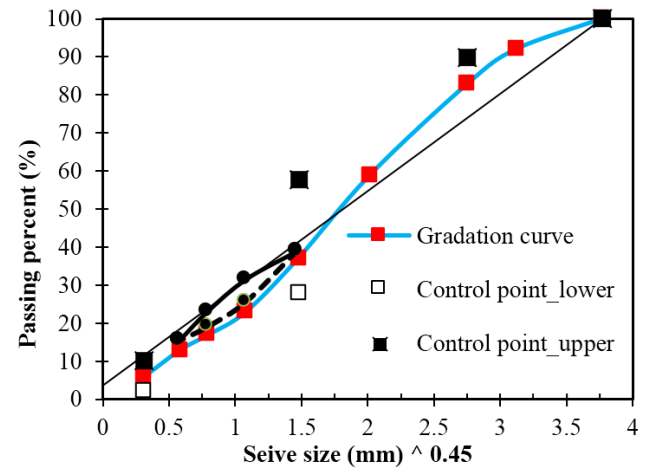


Fig. 1. Aggregate gradation curve of mixtures.

### 3. Test Specimen

#### 3.1. Geometry of Test Specimen

Different test specimens such as disk-shaped compact tension [35, 36], single edge notched beam [37, 38], and Semi-Circular Bending (SCB) [19, 39-42] have been employed in recent years to explore the fracture resistance of asphalt mixtures.

Table 1

Mixture composition and volumetric parameters of each mixture.

Mixture	Mixture composition	V <sub>a</sub> (%)	P <sub>b</sub> (%)	VMA (%)	VFB (%)	G <sub>mm</sub> (g/cm <sup>3</sup> )	Dust/bitumen (%)	Bitumen replacement (%)
HMA	Virgin aggregates +Bitumen 60/70	4	5.3	16.33	69.2	2.316	0.88	0
WMA	Virgin aggregates +Bitumen 60/70 +3% Sasobit	4	5.6	16.1	74.98	2.328	0.93	0
WMA+RAP	Virgin aggregates +25%RAP +Bitumen 60/70 +3% Sasobit	4	6.1	15.3	72.07	2.345	1.01	19.8

V<sub>a</sub>: Percentage of the air voids in the total mixture; P<sub>b</sub>: Optimum bitumen content by mass of the total mixture; VMA: Voids in mineral aggregates; VFB: Voids filled with bitumen; G<sub>mm</sub>: Maximum specific gravity; bitumen replacement: bitumen in RAP/total bitumen in the mixture.

Table 2

Properties of the bitumen used in this research [20, 22].

Property	Test standard	value
Density at 25°C	ASTM D70	1.018
Flash point (°C)	ASTM D92	290
Penetration test at 25°C (0.1mm)	ASTM	D5 62
Ductility (cm)	ASTM D113	130
Softening point (°C)	ASTM D2398	48.5
Viscosity test at 135°C (0.01 st)	ASTM D2170	364
Viscosity test at 165°C (0.01 st)	ASTM D2170	78

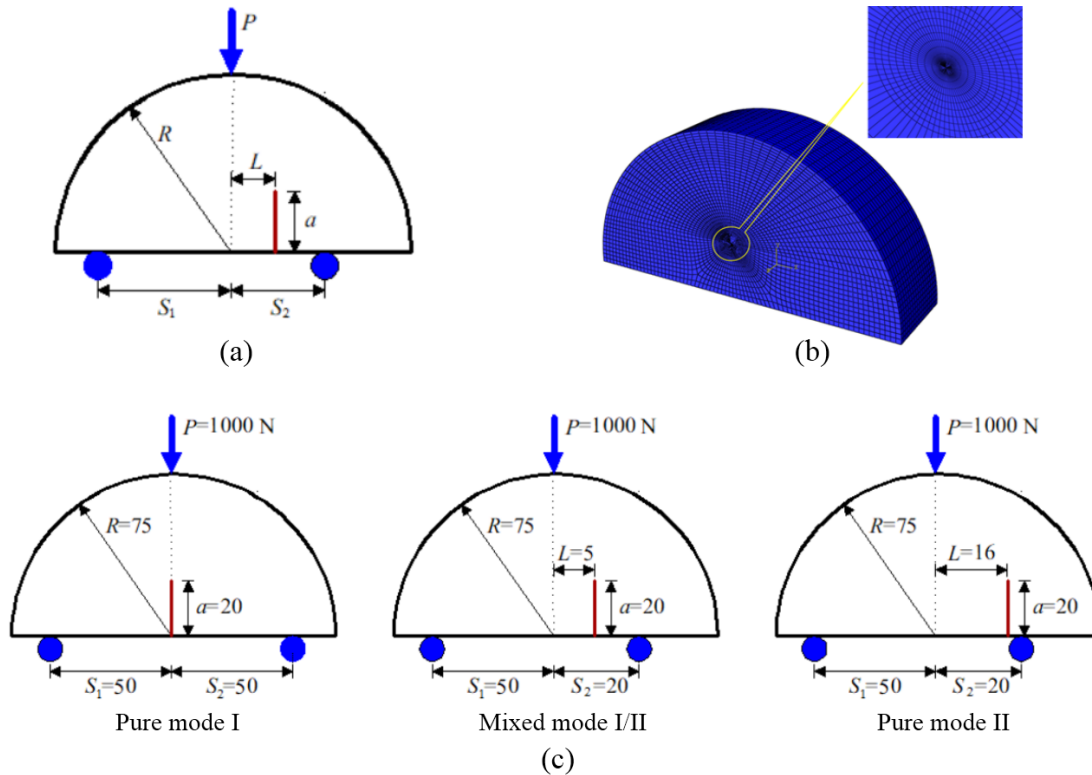


**Fig. 2.** a) Geometry of the SCB specimen, b) Meshing of the SCB specimen, c) Dimensions of the SCB specimen and loading conditions

**Table 3**  
Finite element results for the SCB specimen.

Mode of loading	$M^e$	$S_1, S_2, L$ (mm)	$K_I$ (MPa $\sqrt{m}$ )	$K_{II}$ (MPa $\sqrt{m}$ )	$Y_I$	$Y_{II}$
Pure mode I	1	50, 50, 0	0.195	0	4.8	0
Mixed mode I/II	0.5	50, 20, 5	0.067	0.041	1.28	1.78
Pure mode II	0	50, 20, 16	0	0.122	0	2.33

In this research study, the SCB specimen illustrated in Fig. 2a is employed because it can be simply produced from cylinders manufactured by the gyratory and Marshal compactor machines. It is noticed that this specimen was proposed by Ayatollahi et al. [43], and initially used by Ameri et al. [44] to obtain the fracture toughness of asphalt mixtures. According to Fig. 2a, the SCB specimen containing an edge crack of length  $a$  is placed on the two bottom supports located at  $S_1$  and  $S_2$ , and a load of  $P$  is applied at the top point of the SCB specimen. Another advantage of the SCB specimen is that all the modes of loading including pure mode I, pure mode II and any mixed mode I/II can be easily produced by changing the location of crack  $L$  (see Fig. 2a). Finite element analysis is performed on the SCB specimen shown in Fig. 2a using ABAQUS, and the results are given in Table 3. Based on the results, the pure mode I is achieved when the specimen is loaded symmetrically (i.e. when  $S_1 = S_2 = 50\text{mm}$ ) and the crack is located in the middle ( $L = 0$ ). Whereas, the mixed mode I/II and pure mode II are produced when the specimen is loaded asymmetrically (i.e. when  $S_1 = 50\text{mm}$  and  $S_2 = 20\text{mm}$ ) and the crack is located at a certain distance from the middle. According to

Table 3, as the crack goes away from the middle (i.e. as  $L$  increases), the magnitude of mode II deformation at the crack tip increases, while the portion of mode I decreases. In other words, the specimen is subjected to mixed mode I/II loading. Meanwhile, further movement of the crack location (i.e. when  $L = 16\text{mm}$ ) causes the specimen to be loaded under pure mode II.

In the analysis of SCB specimen using ABAQUS, the elements surrounding the crack tip are assumed as singular elements. Meanwhile, the elements close to the crack tip are considered fine enough to increase the accuracy of the results (i.e. stress intensity factors,  $K_I$  and  $K_{II}$ ), while farther elements are considered coarse. Fig. 2b shows the meshing of the SCB specimen. It is also pointed out that dimensions of the SCB specimen together with the loading conditions (for different modes of loading) considered in the finite element analyses are presented in Fig. 2c. Furthermore, Young's modulus and Poisson's ratio are assumed as  $E = 12.5\text{GPa}$  and  $\nu = 0.35$ , respectively [45]. It is noticed that according to an investigation performed by Pirmohammad and Bayat [21], the values of mechanical properties do not affect the results of finite element presented in Table 3.

$M^e$  given in Table 3 expresses the contribution of mode I and II at the crack tip, which can be defined as follows [44]:

$$M^e = \frac{2}{\pi} \tan^{-1} \left( \frac{K_I}{K_{II}} \right) \quad (1)$$

where,  $K_I$  and  $K_{II}$  are the mode I stress intensity factor and mode II stress intensity factor, respectively, and are extracted from ABAQUS.  $M^e = 0$  and  $M^e = 1$  correspond to the pure mode II and pure mode I, respectively. While, any value of  $M^e$  between 0 and 1 corresponds to mixed mode I/II loading. Likewise, the mode I and mode II geometry factors (i.e.  $Y_I$  and  $Y_{II}$ ) given in Table 3 can be obtained from the following equations [44]:

$$Y_I = \frac{K_I}{\sqrt{\pi a}} \frac{2Rt}{P} \quad (2)$$

$$Y_{II} = \frac{K_{II}}{\sqrt{\pi a}} \frac{2Rt}{P} \quad (3)$$

It is worth noting that the values of  $Y_I$  and  $Y_{II}$  would be used in the subsequent sections for calculating the fracture toughness.

### 3.2. Preparation of Test Specimen

The asphalt mixtures mentioned above are compacted in the laboratory using the SGC (Superpave Gyratory Compactor) machine to generate cylindrical samples with 150mm in diameter and 160mm in height. The bottom and top parts of the cylindrical samples are cut and discarded because of existing large variation of density gradient compared to the other parts of the specimen. Each of the cylinders is then cut into three discs with 30mm in thickness, and thereafter they are halved to prepare six semicircles. An edge crack with 20mm in length is finally created within the semicircles at the places given in Table 3 by means of a cutting machine to produce the SCB specimens. Fig. 3 displays the steps of preparing the SCB specimens.



Fig. 3. Steps of producing SCB specimens.

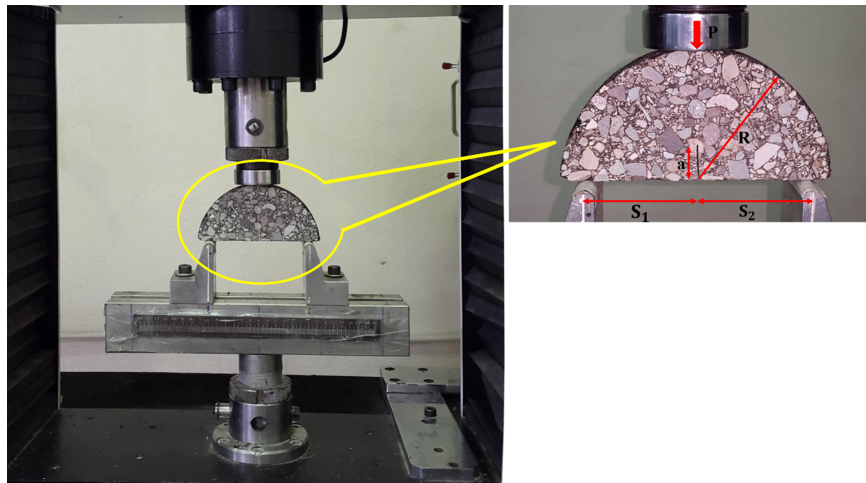


Fig. 4. Fracture test set-up used for measuring the fracture parameters.

#### 4. Fracture Test Procedure

Fracture tests are performed on the SCB specimens made of the three mixtures including HMA, WMA and WMA-RAP under pure mode I, pure mode II and mixed mode loadings. In addition, the experiments are carried out at two different temperatures of  $-15^{\circ}\text{C}$  and  $25^{\circ}\text{C}$ .

A universal test machine is used for performing the tests (see Fig. 4). Prior to performing the tests, the SCB specimens are maintained in a freezer set at the test temperature (i.e.  $-15^{\circ}\text{C}$  or  $25^{\circ}\text{C}$ ) for 4 hours to achieve a uniform temperature within the specimens. The temperature of the environmental chamber is controlled within  $\pm 1^{\circ}\text{C}$  of the desired value. Each of the SCB specimens is then placed upon the bottom supports of the three-point bend fixture adjusted at the proper locations given in Table 3 (i.e.  $S_1$  and  $S_2$ ). Afterwards, the cross-head (i.e. the upper support of the fixture) is lowered with a speed of  $1\text{mm}/\text{min}$  to load the SCB specimen. Load (i.e.  $F$ ) and cross-head displacement (i.e.  $V$ ) is recorded throughout the test. Fig. 5 exhibits samples of the load versus cross-head displacement ( $F - V$ ) curves, as the test results.

The bottom supports are set at  $S_1 = 50\text{mm}$  &  $S_2 = 50\text{mm}$  for the pure mode I, and  $S_1 = 50\text{mm}$  &  $S_2 = 20\text{mm}$  for the pure mode II and mixed modes of I/II tests. Meanwhile, the crack location within the SCB specimens for the experiments under different modes of loading has been presented in Table 1. It is also pointed out that each case of the experiments is repeated three times to increase the precision of the results.

#### 5. Data Processing Using Fracture Mechanics

Two parameters of fracture toughness and fracture energy are calculated from the experimental data ob-

tained from the fracture tests carried out under various loading modes at the test temperatures of  $-15^{\circ}\text{C}$  or  $25^{\circ}\text{C}$ .

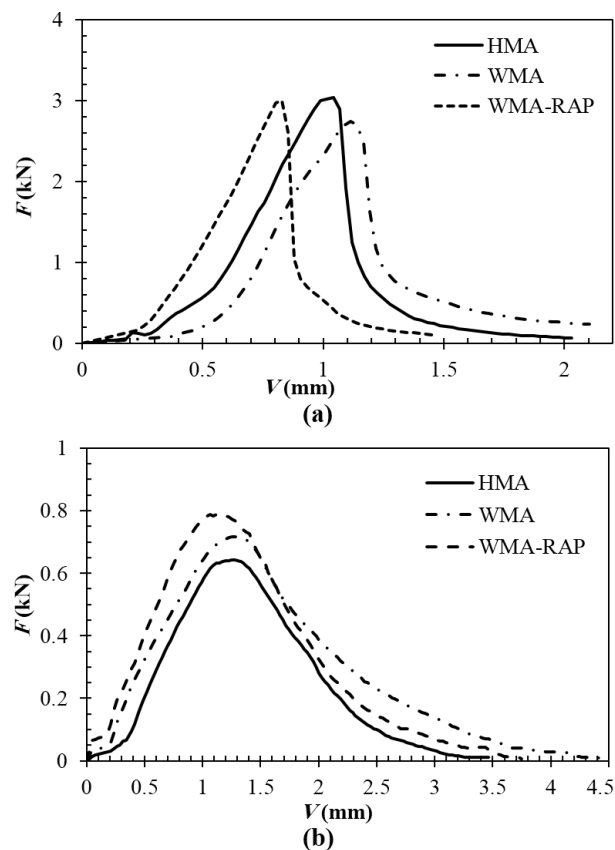


Fig. 5. Samples of  $F - V$  curves recorded from the tests performed at a)  $-15^{\circ}\text{C}$  and b)  $25^{\circ}\text{C}$

##### 5.1. Fracture Toughness

Fracture toughness (i.e.  $K_f$ ) represents the material resistance against the initiation of crack growth. In general, the fracture toughness depends on the dimensions of test specimen, loading condition, length of

crack, and critical load obtained from the test. This parameter (i.e.  $K_f$ ) is written as follows [44]:

$$K_f = \sqrt{(K_{If}^2 + K_{IIIf}^2)} \tag{4a}$$

$$K_{If} = Y_I \frac{F_{cr}}{2Rt} \sqrt{\pi a} \tag{4b}$$

$$K_{IIIf} = Y_{II} \frac{F_{cr}}{2Rt} \sqrt{\pi a} \tag{4c}$$

where,  $R$ ,  $t$  and  $a$  are the radius, thickness and crack length. In addition,  $K_{If}$ ,  $K_{IIIf}$ ,  $Y_I$  and  $Y_{II}$  are the mode I critical SIF (Stress Intensity Factor), mode II

critical SIF, mode I geometry factor and mode II geometry factor, respectively. It is reminded that the geometry factors (i.e.  $Y_I$  and  $Y_{II}$ ) are obtained from the numerical simulations, as discussed earlier. Meanwhile, the parameter  $F_{cr}$  is called the critical load, and is calculated as the maximum load present in  $F - V$  curve. The values of  $F_{cr}$  for the mixtures of HMA, WMA and WMA-RAP under various loading modes at  $-15^\circ\text{C}$  and  $25^\circ\text{C}$  are shown in Table 4. Furthermore, the values of fracture toughness are computed by putting the values of  $F_{cr}$  into Eq. (4), which are given in Table 5.

**Table 4**

Critical load  $F_{cr}$  (kN), SD and COV for the asphalt mixtures subjected to different modes of loading at the temperatures of a)  $-15^\circ\text{C}$ , and b)  $25^\circ\text{C}$ .

(a)					
$M^e$		Test No.	HMA	WMA	WMA-RAP
1		1	2.865	3.693	3.683
		2	2.664	3.576	3.768
		3	3.039	3.637	3.920
	Average		2.856	3.636	3.791
	SD		0.190	0.058	0.120
	COV		6.56	1.61	3.16
0.5		1	5.503	7.225	7.030
		2	5.599	6.244	8.767
		3	4.619	6.905	8.377
	Average		5.241	6.791	8.058
	SD		0.540	0.500	0.911
	COV		10.31	7.37	11.30
0		1	5.408	6.596	8.096
		2	5.565	6.949	7.916
		3	5.490	6.063	8.211
	Average		5.488	6.536	8.075
	SD		0.079	0.446	0.149
	COV		1.44	6.83	1.84
(b)					
$M^e$		Test No.	HMA	WMA	WMA-RAP
1		1	0.644	0.633	0.790
		2	0.614	0.717	0.670
		3	0.530	0.687	0.723
	Average		0.596	0.679	0.728
	SD		0.059	0.043	0.061
	COV		9.91	6.27	8.26
0.5		1	0.983	1.552	1.666
		2	1.109	1.637	1.948
		3	0.916	1.887	2.002
	Average		1.003	1.692	1.872
	SD		0.098	0.174	0.181
	COV		9.78	10.29	9.64
0		1	0.954	1.466	1.772
		2	0.894	1.692	1.706
		3	0.994	1.700	1.871
	Average		0.947	1.619	1.783
	SD		0.051	0.133	0.083
	COV		5.31	8.20	4.66

**Table 5**

The values of  $K_{If}$ ,  $K_{IIIf}$  and  $K_f$  for the mixtures of HMA, WMA and WMA-RAP under different modes of loading at a)  $-15^\circ\text{C}$ , and b)  $25^\circ\text{C}$ .

(a)

$M^e$	Test No.	HMA			WMA			WMA-RAP		
		$K_{IF}$	$K_{IIIf}$	$K_f$	$K_{If}$	$K_{IIIf}$	$K_f$	$K_{If}$	$K_{IIIf}$	$K_f$
1	1	0.72	0	0.72	0.93	0	0.93	0.92	0	0.92
	2	0.67	0	0.67	0.90	0	0.90	0.94	0	0.94
	3	0.76	0	0.76	0.91	0	0.91	0.98	0	0.98
	Average	0.72	0	0.72	0.91	0	0.91	0.95	0	0.95
0.5	1	0.37	0.51	0.63	0.48	0.67	0.83	0.47	0.65	0.80
	2	0.37	0.52	0.64	0.42	0.58	0.71	0.59	0.81	1.00
	3	0.31	0.43	0.53	0.46	0.64	0.79	0.56	0.78	0.96
	Average	0.35	0.49	0.60	0.50	0.70	0.78	0.54	0.75	0.92
0	1	0	0.66	0.66	0	0.80	0.80	0	0.98	0.98
	2	0	0.68	0.68	0	0.84	0.84	0	0.96	0.96
	3	0	0.67	0.67	0	0.74	0.74	0	1.00	1.00
	Average	0	0.67	0.67	0	0.79	0.79	0	0.98	0.98

(b)

$M^e$	Test No.	HMA			WMA			WMA-RAP		
		$K_{IF}$	$K_{IIIf}$	$K_f$	$K_{If}$	$K_{IIIf}$	$K_f$	$K_{If}$	$K_{IIIf}$	$K_f$
1	1	0.16	0	0.16	0.22	0	0.22	0.30	0	0.30
	2	0.15	0	0.15	0.18	0	0.18	0.22	0	0.22
	3	0.13	0	0.13	0.21	0	0.21	0.23	0	0.23
	Average	0.15	0	0.15	0.21	0	0.21	0.25	0	0.25
0.5	1	0.07	0.09	0.11	0.10	0.14	0.18	0.11	0.15	0.19
	2	0.07	0.10	0.13	0.11	0.15	0.19	0.13	0.18	0.22
	3	0.06	0.09	0.10	0.13	0.18	0.22	0.13	0.19	0.23
	Average	0.07	0.09	0.11	0.11	0.16	0.19	0.13	0.17	0.21
0	1	0	0.12	0.12	0	0.18	0.18	0	0.21	0.21
	2	0	0.11	0.11	0	0.23	0.23	0	0.21	0.21
	3	0	0.12	0.12	0	0.21	0.21	0	0.23	0.23
	Average	0	0.12	0.12	0	0.20	0.20	0	0.22	0.22

## 5.2. Fracture Energy

Fracture energy ( $G_f$ ) is another fundamental parameter for fracture property of materials. This parameter takes into account both the crack initiation (i.e. before critical load in  $F-V$  curve) and crack propagation (i.e. after critical load in  $F-V$  curve) during the fracture process. The fracture energy is computed from the following equation as per RILEM TC 50-FMC specification that is widely utilized in concretes [46].

$$G_f = \frac{W_f}{A_{lig}} \quad (5)$$

where,  $W_f$  is the work of fracture, and is calculated as the area under the  $F-V$  curve. In addition,  $A_{lig}$  refers to the area of the ligament that is the product of the ligament length and the thickness of the SCB specimen. It is worth noting that in order to calculate the ligament length of the specimen, a string is placed on the crack path at the front side of the specimen, and its length is then measured. This process is repeated for the back side of the specimen. The mea-

sured lengths are finally averaged. It is pointed out that the crack path has been assumed as a straight line in the previous investigations (see e.g. [47-49]), which is not accurate enough because the fracture surface of asphalt mixtures is not smooth. Hence, the procedure proposed in the current research for calculating the ligament area (i.e.  $A_{lig}$ ) is more precise than that used by other researchers.

## 6. Results and Discussion

As mentioned earlier, fracture tests were conducted on the SCB specimens made of HMA, WMA and WMA-RAP under various loading modes at  $-15^\circ\text{C}$  and  $25^\circ\text{C}$ . The fracture loads (i.e.  $F_{cr}$ ) obtained from the tests were given in Table 4. The Standard Deviation (SD) and Coefficient of Variations (COVs) of the fracture loads are calculated as presented in Table 4. According to this Table, the values of SD and COVs are very small, and the values of COVs are smaller than 6%. This indicates that the results of experiments are very near to the average value of  $F_{cr}$ . Consequently, re-

peatability of the experiments carried out in this research is satisfactory. Based on the results given in Table 4, the fracture loads for the mixtures made of Sasobit are higher than those for the mixtures made of plain bitumen; because, Sasobit forms a crystalline network and therefore increases the stiffness of mixtures [50]. Furthermore, the fracture load increases with the addition of RAP to WMA mixture for any mode of loading; because, the aged bitumen present in RAP increases the stiffness of asphalt mixture [50].

Fig. 6 shows the results of fracture toughness and fracture energy calculated for the mixtures of HMA, WMA and WMA-RAP at  $-15^{\circ}\text{C}$ . According to Fig. 6a, the WMA and WMA-RAP concretes provide higher fracture toughness than the HMA concrete under any mode of loading. In addition, the WMA-RAP mixture shows the highest value of fracture toughness.

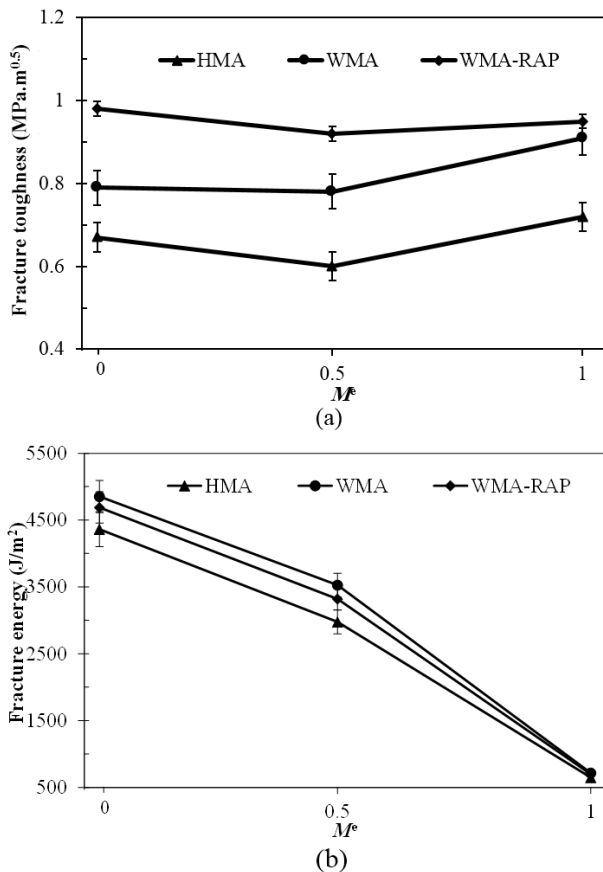


**Fig. 6.** a) Fracture toughness, and b) Fracture energy of asphalt mixtures under different modes of loading at  $-15^{\circ}\text{C}$ .

Indeed, the addition of Sasobit to bitumen reduces the penetration grade [51], and therefore increases the strength of mixture. On the other hand, the RAP imparts additional strength to the mixture, which increases the mixture resistance against the initiation of crack. Meanwhile, the fracture toughness generally reduces and then enhances as the amount of mode II increases. This behavior is similar to the results of previous researches (see e.g. [18, 22, 52]).

According to Fig. 6b, the WMA and WMA-RAP concretes resist better than the HMA against the crack propagation under any mode of loading at  $-15^{\circ}\text{C}$ ; however, the WMA concrete shows the highest fracture energy amongst the concretes investigated at the current study. Although the Sasobit present in WMA and WMA-RAP concretes has a positive effect on the enhancement of fracture energy, the addition of RAP to WMA concrete leads to the reduction of fracture energy. Indeed, asphalt mixtures behave in brittle manner at low temperatures, and the addition of RAP increases brittleness of the mixture; hence, the mixture of WMA-RAP is expected to show lower fracture resistance against the crack propagation compared to the mixture of WMA.

For all the mixtures considered in this research, the fracture energy increases as the shear mode enhances, indicating that more energy is required for the crack propagation by enhancing the shear mode. It is also noticed that the fracture energy of concretes is approximately the same when they are subjected to the pure mode I loading; while, the effect of Sasobit (which exists in the WMA and WMA-RAP mixtures) is more pronounced for the shear loadings.

Based on Fig. 7a, the trend of results at  $25^{\circ}\text{C}$  is similar to that at  $-15^{\circ}\text{C}$  i.e. the mixtures of WMA and WMA-RAP demonstrate greater fracture toughness than the HMA, and the WMA-RAP mixture exhibits the highest value of fracture toughness. In addition, according to Fig. 7b, the mixtures containing Sasobit (i.e. WMA and WMA-RAP) show higher fracture energy than the HMA mixture under any mode of loading. However, the WMA mixture has the highest fracture energy compared with the other mixtures. An important result from Fig. 7b is that unlike the results of fracture energy at the test temperature of  $-15^{\circ}\text{C}$ , the mode II fracture energy is less than the mixed mode fracture energy at  $25^{\circ}\text{C}$  for all the mixtures.

The effect of temperature on the fracture performance of mixtures is shown in Fig. 8, in which all the mixtures of HMA, WMA and WMA-RAP demonstrate higher values of the fracture toughness and fracture energy at  $-15^{\circ}\text{C}$  than those at  $25^{\circ}\text{C}$ . Because, both the bitumen strength and the adhesion between aggregate and bitumen increase as the temperature reduces [1, 53].

According to Fig. 8, the fracture toughness at both the test temperatures of  $-15^{\circ}\text{C}$  and  $25^{\circ}\text{C}$  are slightly dependent on the loading mode; while, the fracture energies at these temperatures are highly dependent on the mode of loading. In other words, the pure mode I fracture energies at  $-15^{\circ}\text{C}$  and  $25^{\circ}\text{C}$  are nearly the same; whereas, the difference in the results of fracture energy at  $-15^{\circ}\text{C}$  and  $25^{\circ}\text{C}$  increases as the amount of shear mode enhances (i.e. as  $M^e$  decreases). Hence, the effect of temperature on the fracture energy of asphalt mixtures is more pronounced when they are subjected to the pure mode II loading.

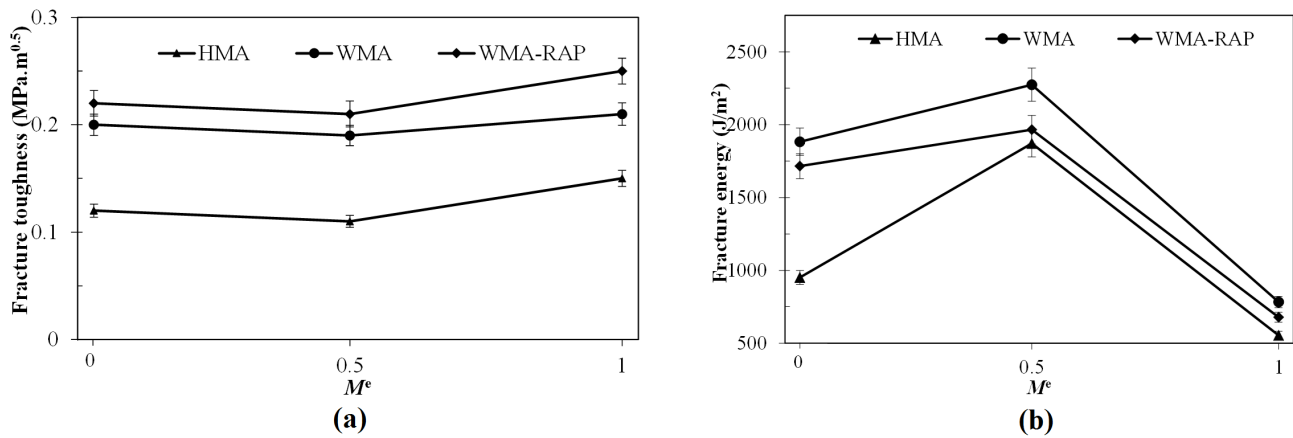


Fig. 7. a) Fracture toughness, and b) Fracture energy of asphalt mixtures under different modes of loading at 25°C.

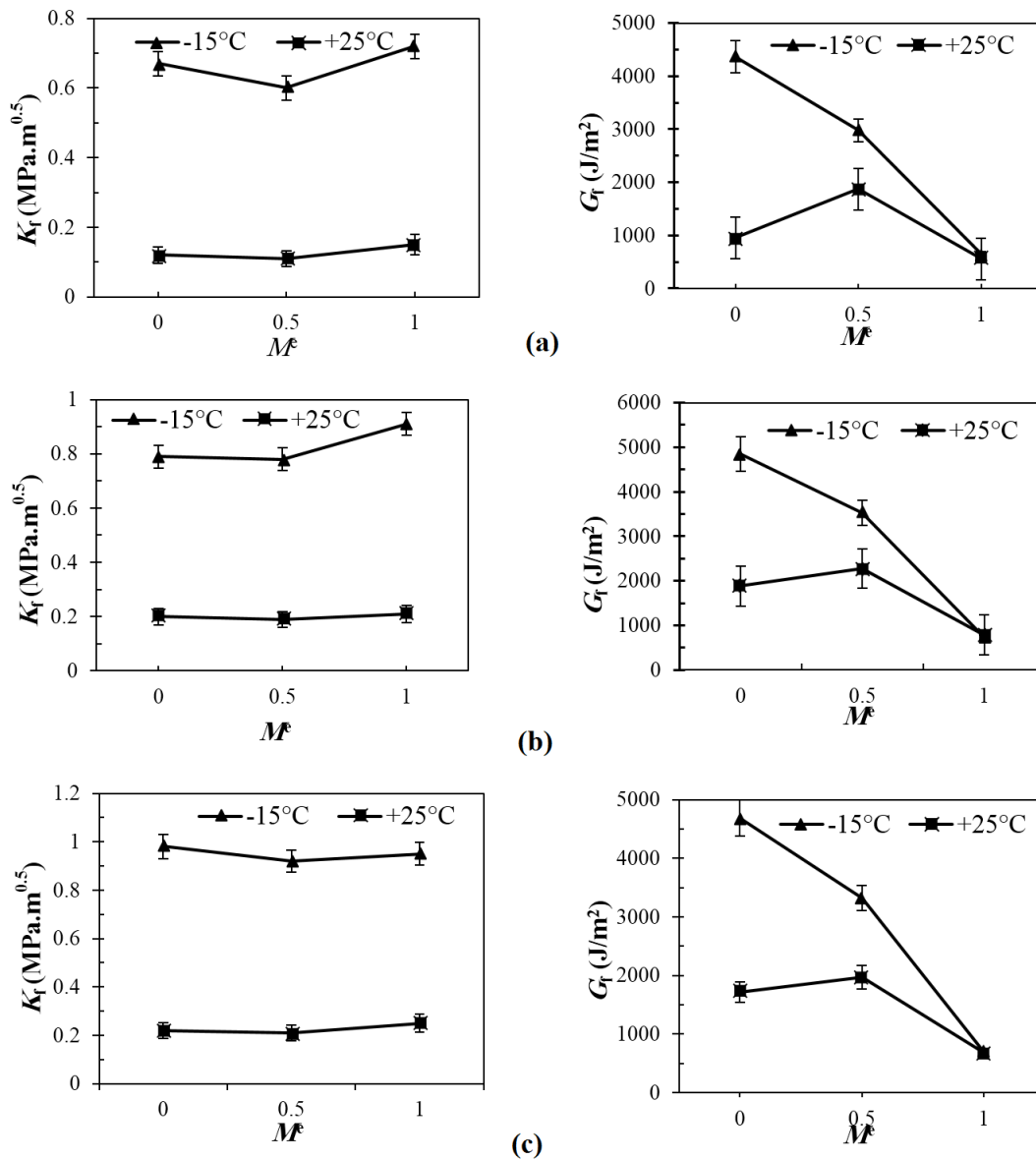
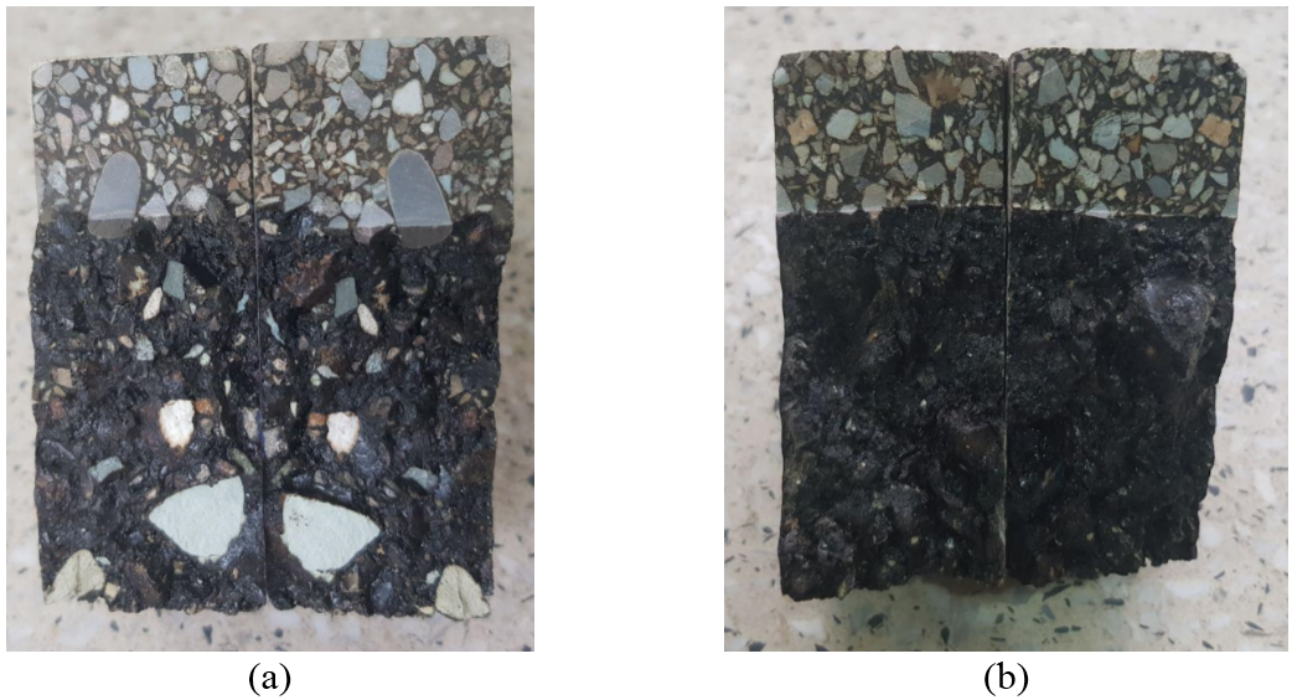


Fig. 8. Variations of fracture parameters versus  $M^e$  for the mixtures of a) HMA, b) WMA, c) WMA-RAP at different temperatures.



**Fig. 9.** Fracture surface of SCB specimens observed at the test temperatures of a)  $-15^{\circ}\text{C}$  and b)  $25^{\circ}\text{C}$ .

From the results mentioned above, it can be concluded that although WMA mixtures are produced at temperatures  $20\text{--}55^{\circ}\text{C}$  lower than HMA ones, the fracture performance of WMA is better than HMA mixture. Particularly, the WMA-RAP mixture which contains the RAP material shows more promising results in terms of fracture resistance against the fracture.

A brittle fracture has occurred during the tests performed at  $-15^{\circ}\text{C}$  because the crack has propagated through the aggregates (i.e. by breaking the aggregates), as shown in Fig. 9. Whereas, at the experiments carried out at  $25^{\circ}\text{C}$ , the crack has propagated around the aggregates (i.e. at the interface between the aggregates and bitumen).

## 7. Summary and Conclusions

In this research, fracture properties including the fracture toughness and fracture energy of three various mixtures (i.e. HMA, WMA and WMA-RAP) are measured. For this purpose, fracture experiments are performed using the SCB specimen under three different modes of loading (i.e. pure mode I, pure mode II and mixed mode I/II) at the test temperatures of  $-15^{\circ}\text{C}$  and  $25^{\circ}\text{C}$ . The results of this research study are summarized as follows:

- The values of SD and COVs were very small, indicating that the results of experiments (i.e.  $F_{cr}$ ) were very near together. Consequently, the repeatability of the experiments was satisfactory.
- WMA and WMA-RAP mixtures provided better fracture properties (i.e. fracture toughness

and fracture energy) than the HMA mixture under any mode of loading at both temperatures of  $-15^{\circ}\text{C}$  and  $25^{\circ}\text{C}$ . Meanwhile, the WMA-RAP and WMA mixtures showed the highest values of fracture toughness and fracture energy, respectively as compared with other mixtures.

- At both test temperatures of  $-15^{\circ}\text{C}$  and  $25^{\circ}\text{C}$ , the fracture toughness initially decreased and then increased as the proportion of mode II relative to mode I enhanced.
- At the test temperature of  $-15^{\circ}\text{C}$ , the fracture energy of mixtures increased as the shear mode enhanced (i.e. as  $M^e$  decreased). Whereas, by enhancing the shear mode, the fracture energy of mixtures increased and then decreased at the test temperature of  $25^{\circ}\text{C}$ .
- Both the fracture toughness and fracture energy of the mixtures at  $-15^{\circ}\text{C}$  were higher than those at  $25^{\circ}\text{C}$ .
- Crack propagated through the aggregates at the low temperature of  $-15^{\circ}\text{C}$ ; while, it extended around the aggregates (i.e. at the interface between aggregates and bitumen) at the intermediate temperature of  $25^{\circ}\text{C}$ .

## References

- [1] S. Pirmohammad, M.R. Ayatollahi, Fracture Behavior of Asphalt Materials, 1 ed., Springer International Publishing, (2020).

- [2] C. Hettiarachchi, X. Hou, J. Wang, F. Xiao, A comprehensive review on the utilization of reclaimed asphalt material with warm mix asphalt technology, *Constr. Build. Mater.*, 227 (2019) 117096.
- [3] M. Sabouri, T. Bennert, J. Sias Daniel, Y. Richard Kim, A comprehensive evaluation of the fatigue behaviour of plant-produced RAP mixtures, *Road Mater. Pavement Des.*, 16(sup 2) (2015) 29-54.
- [4] B. Golchin, A. Mansourian, Evaluation of fatigue properties of asphalt mixtures containing reclaimed asphalt using response surface method, *Int. J. Transp. Eng.*, 4(4) (2017) 335-350.
- [5] P.C. Boriack, S.W. Katicha, G.W. Flintsch, C.R. Tomlinson, Laboratory evaluation of asphalt concrete mixtures containing high contents of reclaimed asphalt pavement (RAP) and binder, Virginia Center for Transportation Innovation and Research, (2014).
- [6] D. Vukosavljevic, Fatigue characteristics of field HMA surface mixtures containing recycled asphalt pavement (RAP), MSc Thesis, Civil Engineering Department, Tennessee: University of Tennessee, (2006).
- [7] U.A. Mannan, M.R. Islam, R.A. Tarefder, Effects of recycled asphalt pavements on the fatigue life of asphalt under different strain levels and loading frequencies, *Int. J. Fatigue*, 78 (2015) 72-80.
- [8] S. Mangiafico, C. Sauzéat, H. Di Benedetto, S. Pouget, F. Olard, L. Planque, R. Van Rooijen, Statistical analysis of influence of mix design parameters on mechanical properties of mixes with reclaimed asphalt pavement, *Transp. Res. Rec.*, 2445(1) (2014) 29-38.
- [9] N. Guo, Z. You, Y. Tan, Y. Zhao, Performance evaluation of warm mix asphalt containing reclaimed asphalt mixtures, *Int. J. Pavement Eng.*, 18(11) (2017) 981-989.
- [10] D.X. Lu, M. Saleh, Laboratory evaluation of warm mix asphalt incorporating high RAP proportion by using evotherm and sylvaroad additives, *Constr. Build. Mater.*, 114 (2016) 580-587.
- [11] M. Fakhri, A. Ahmadi, Evaluation of fracture resistance of asphalt mixes involving steel slag and RAP: Susceptibility to aging level and freeze and thaw cycles, *Constr. Build. Mater.*, 157 (2017) 748-756.
- [12] A. Behroozikhah, S.H. Morafa, S. Aflaki, Investigation of fatigue cracks on RAP mixtures containing Sasobit and crumb rubber based on fracture energy, *Constr. Build. Mater.*, 141 (2017) 526-532.
- [13] B. Behnia, S. Ahmed, E.V. Dave, W.G. Buttlar, Fracture Characterization of Asphalt Mixtures with Reclaimed Asphalt Pavement, *Int. J. Pavement Res. Technol.*, 3(2) (2010) 72-78.
- [14] M. Mubaraki, S.A. Osman, H.E.M. Sallam, Effect of RAP content on flexural behavior and fracture toughness of flexible pavement, *Lat. Am. J. Solids Stru.*, 16(3) (2019) e177.
- [15] B. Huang, Z. Zhang, W. Kingery, G. Zuo, Fatigue crack characteristics of HMA mixtures containing RAP, *Proceeding 5th Int. Conf. on Cracking in Pavements, RILEM, Limoges, France, (2004) 631-638.*
- [16] H. Ziari, A. Amini, A. Moniri, M. Habibpour, Using the GMDH and ANFIS methods for predicting the crack resistance of fibre reinforced high RAP asphalt mixtures, *Road Mater. Pavement Des.*, (2020), DOI: 10.1080/14680629.2020.1748693.
- [17] X.J. Li, M.O. Marasteanu, Using semi circular bending test to evaluate low temperature fracture resistance for asphalt concrete, *Exp. Mech.*, 50(7) (2010) 867-876.
- [18] S. Pirmohammad, M.R. Ayatollahi, Fracture resistance of asphalt concrete under different loading modes and temperature conditions, *Constr. Build. Mater.*, 53 (2014) 235-242.
- [19] S. Pirmohammad, H. Khoramishad, M.R. Ayatollahi, Effects of asphalt concrete characteristics on cohesive zone model parameters of hot mix asphalt mixtures, *Can. J. Civ. Eng.*, 43(3) (2016) 226-232.
- [20] S. Pirmohammad, H. Shabani, Mixed mode I/II fracture strength of modified HMA concretes subjected to different temperature conditions, *J. Test. Eval.*, 47(5) (2019) 3355-3371.
- [21] S. Pirmohammad, A. Bayat, Fracture resistance of HMA mixtures under mixed mode I/III loading at different subzero temperatures, *Int. J. Solids Struct.*, 120 (2017) 268-277.
- [22] M.R.M. Aliha, H. Fazaali, S. Aghajani, F. Moghadas Nejad, Effect of temperature and air void on mixed mode fracture toughness of modified asphalt mixtures, *Constr. Build. Mater.*, 95 (2015) 545-555.
- [23] M.R.M. Aliha, On predicting mode II fracture toughness ( $K_{IIc}$ ) of hot mix asphalt mixtures using the strain energy density criterion, *Theor. Appl. Fract. Mech.*, 99 (2019) 36-43.
- [24] A. Razmi, M. Mirsayar, Fracture resistance of asphalt concrete modified with crumb rubber at low temperatures, *Int. J. Pavement Res. Technol.*, 11(3) (2018) 265-273.

- [25] S. Pirmohammad, Y. Majd-Shokorlou, B. Amani, Experimental investigation of fracture properties of asphalt mixtures modified with Nano  $\text{Fe}_2\text{O}_3$  and carbon nanotubes, *Road Mater. Pavement Des.*, 21(8) (2020) 2321-2343.
- [26] S. Pirmohammad, Y. Majd-Shokorlou, B. Amani, Fracture resistance of HMA mixtures modified with nanoclay and Nano- $\text{Al}_2\text{O}_3$ , *J. Test. Eval.*, 47(5) (2019) 3289-3308.
- [27] H. Ziari, H. Farahani, A. Goli, S. Sadeghpour Galooyak, The investigation of the impact of carbon nano tube on bitumen and HMA performance, *Pet. Sci. Technol.*, 32(17) (2014) 2102-2108.
- [28] A. Mansourian, A. Razmi, M. Razavi, Evaluation of fracture resistance of warm mix asphalt containing jute fibers, *Constr. Build. Mater.*, 117 (2016) 37-46.
- [29] M.R.M. Aliha, A. Razmi, A. Mansourian, The influence of natural and synthetic fibers on low temperature mixed mode I+ II fracture behavior of warm mix asphalt (WMA) materials, *Eng. Fract. Mech.*, 182 (2017) 322-336.
- [30] S. Pirmohammad, Y. Majd Shokorlou, B. Amani, Laboratory investigations on fracture toughness of asphalt concretes reinforced with carbon and kenaf fibers, *Eng. Fract. Mech.*, 226 (2020) 106875.
- [31] S. Pirmohammad, Y. Majd Shokorlou, B. Amani, Influence of natural fibers (kenaf and goat wool) on mixed mode I/II fracture strength of asphalt mixtures, *Constr. Build. Mater.*, 239 (2020) 117850.
- [32] M. Ameri, H. Ziari, A. Yousefi, A. Behnood, Moisture susceptibility of asphalt mixtures: A thermodynamic evaluation of the effects of anti-stripping additives, *J. Mater. Civ. Eng.*, In Press (2020).
- [33] ASTM D2172, Standard Test Methods for Quantitative Extraction of Asphalt Binder from Asphalt Mixtures, ASTM International, West Conshohocken, PA, USA, (2017).
- [34] ASTM D5404/D5404M-12, Standard Practice for Recovery of Asphalt from Solution Using the Rotary Evaporator, ASTM International, West Conshohocken, PA, USA, (2017).
- [35] M. Wagoner, W.G. Buttlar, G. Paulino, Disk-shaped compact tension test for asphalt concrete fracture, *Exp. Mech.*, 45(3) (2005) 270-277.
- [36] M. Wagoner, W. Buttlar, G. Paulino, P. Blankenship, Investigation of the fracture resistance of hot-mix asphalt concrete using a disk-shaped compact tension test, *Transp. Res. Rec. Transp. Res. Rec.*, (1929) (2005) 183-192.
- [37] B. Mobasher, M.S. Mamlouk, H.M. Lin, Evaluation of crack propagation properties of asphalt mixtures, *J. Transp. Eng.*, 123(5) (1997) 405-413.
- [38] K.W. Kim, Y.S. Doh, S. Lim, Mode I reflection cracking resistance of strengthened asphalt concretes, *Constr. Build. Mater.*, 13(5) (1999) 243-251.
- [39] J. Molenaar, X. Liu, A. Molenaar, Resistance to crack-growth and fracture of asphalt mixture, 6th International RILEM Symposium, Zurich, Switzerland, 14-16 April, (2003).
- [40] I. Artamendi, H.A. Khalid, A comparison between beam and semi-circular bending fracture tests for asphalt, *Road Mater. Pavement Des.*, 7(sup1) (2006) 163-180.
- [41] M.R. Ayatollahi, S. Pirmohammad, Temperature effects on brittle fracture in cracked asphalt concretes, *Struct. Eng. Mech.*, 45(1) (2013) 19-32.
- [42] M.R.M. Aliha, H. Behbahani, H. Fazaeli, M.H. Rezaifar, Study of characteristic specification on mixed mode fracture toughness of asphalt mixtures, *Constr. Build. Mater.*, 54 (2014) 623-635.
- [43] M.R. Ayatollahi, M.R.M. Aliha, H. Saghafi, An improved semi-circular bend specimen for investigating mixed mode brittle fracture, *Eng. Fract. Mech.*, 78(1) (2011) 110-123.
- [44] M. Ameri, A. Mansourian, S. Pirmohammad, M.R.M. Aliha, M.R. Ayatollahi, Mixed mode fracture resistance of asphalt concrete mixtures, *Eng. Fract. Mech.*, 93 (2012) 153-167.
- [45] D. Timm, B. Birgisson, D. Newcomb, Development of mechanistic-empirical pavement design in Minnesota, *Transp. Res. Rec. Transp. Res. Rec.*, 1629(1) (1998) 181-188.
- [46] R.D. Recommendation, Determination of the fracture energy of mortar and concrete by means of three-point bend tests on notched beams, *Mater. Struct.*, 18(106) (1985) 285-290.
- [47] X. Li, A.F. Braham, M.O. Marasteanu, W.G. Buttlar, R.C. Williams, Effect of factors affecting fracture energy of asphalt concrete at low temperature, *Road Mater. Pavement Des.*, 9(sup1) (2008) 397-416.
- [48] A.F. Braham, W.G. Buttlar, M.O. Marasteanu, Effect of binder type, aggregate, and mixture composition on fracture energy of hot-mix asphalt in cold climates, *Transp. Res. Rec.*, 2001(1) (2007) 102-109.
- [49] S.H. Khanghahi, A. Tortum, Determination of the optimum conditions for gilsonite and glass fiber in HMA under mixed mode I/III loading in fracture tests, *J. Mater. Civ. Eng.*, 30(7) (2018) 04018130.

- [50] S. Sobhi, A. Yousefi, A. Behnood, The effects of Gilsonite and Sasobit on the mechanical properties and durability of asphalt mixtures, *Constr. Build. Mater.*, 238 (2020) 117676.
- [51] H. Fazaeli, Y. Samin, A. Pirnoun, A.S. Dabiri, Laboratory and field evaluation of the warm fiber reinforced high performance asphalt mixtures (case study Karaj–Chaloos Road), *Constr. Build. Mater.*, 122 (2016) 273-283.
- [52] S. Pirmohammad, A. Kiani, Effect of temperature variations on fracture resistance of HMA mixtures under different loading modes, *Mater. Struct.*, 49(9) (2016) 3773-3784.
- [53] K.W. Kim, S.J. Kweon, Y.S. Doh, T.S. Park, Fracture toughness of polymer-modified asphalt concrete at low temperatures, *Can. J. Civ. Eng.*, 30(2) (2003) 406-413.